CHALMERS
UNIVERSITY OF TECHNOLOGY

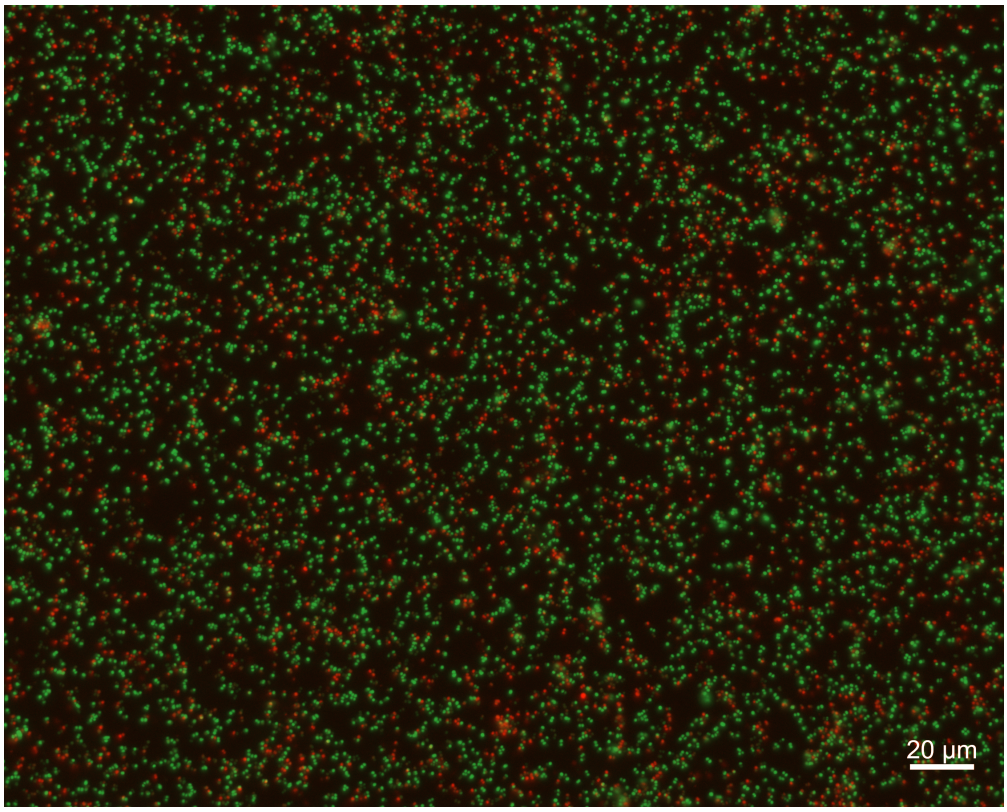

Antibacterial activity of photothermal gold nanorods combined with antimicrobial peptides

Master's thesis in Biotechnology

ALVA NILSSON

DEPARTMENT OF CHEMISTRY and CHEMICAL ENGINEERING
CHALMERS UNIVERSITY OF TECHNOLOGY
Gothenburg, Sweden 2025
www.chalmers.se

Master's thesis 2025

Antibacterial activity of photothermal gold nanorods combined with antimicrobial peptides

ALVA NILSSON

CHALMERS
UNIVERSITY OF TECHNOLOGY

Department of Chemistry and Chemical Engineering
Division of Applied Chemistry
Martin Andersson's group
Chalmers University of Technology
Gothenburg, Sweden 2025

Antibacterial activity of photothermal gold nanorods combined with antimicrobial peptides ALVA NILSSON

Supervisor: Maja Uusitalo, Applied Chemistry
Examiner: Martin Andersson, Applied Chemistry

Master's Thesis 2025
Department of Chemistry and Chemical Engineering
Division of Applied Chemistry
Martin Andersson's group
Chalmers University of Technology
SE-412 96 Gothenburg
Telephone +46 31 772 1000

Cover: Fluorescence microscopy micrograph of LIVE/DEAD® BacLight™ stained *S. aureus* on an AuNR surface after irradiation with NIR light and submersion in AMP suspension

Typeset in LaTeX
Printed by Chalmers Reproservice
Gothenburg, Sweden 2025

Antibacterial activity of photothermal gold nanorods combined with antimicrobial peptides

ALVA NILSSON
Department of Chemistry and Chemical Engineering
Chalmers University of Technology

Abstract

Biomaterials, used in medical implants for example, are important tools in modern medicine to ensure health and quality of life. Despite their benefits, biomaterials currently face two major problems, the difficulty of treating persistent biomaterial-associated infections and the rapid increase in bacterial antimicrobial resistance. It can be concluded that there is an urgent need for development of biomaterials able to prevent biomaterial-associated infections without relying on conventional antibiotics. Promising solutions are the implementation of antibacterial surface modifications of biomaterials and the use of antimicrobial peptides.

The focus of this thesis was to perform *in vitro* evaluation of a material modification combining the antibacterial activity of surfaces functionalised with photothermal gold nanorods (AuNRs) in the presence of antimicrobial peptides (AMPs). The evaluation was performed by antimicrobial susceptibility testing, agar plate models and fluorescence microscopy. Significant antibacterial activity could be observed when irradiating AuNRs with near-infrared light in the presence of AMPs when tested against *Staphylococcus aureus*. A slight synergistic relationship between the AuNRs and AMPs could be observed, but further testing is needed to confirm the effect. This thesis provides important insight into the antibacterial activity of surfaces functionalised with photothermal AuNRs when in the presence of AMPs.

Keywords: biomaterials, biomaterial-associated infections, antimicrobial resistance, *in vitro* evaluation, gold nanorods, near-infrared light, antimicrobial peptides.

Acknowledgements

This thesis would not have been possible without the people that I now want to give proper thanks to. I would like to start by thanking my examiner Martin Andersson for giving me the opportunity to undertake my thesis in your group. I have found this subjects incredibly interesting and fun to work with and greatly appreciate the interest you have shown. I would also like to thank my supervisor Maja Uusitalo for allowing me to contribute to your research and for sharing your knowledge. Despite setbacks during the project, you always had time to explain and discuss your subject, and give lots of encouragement and support. To everyone at the division of Applied Chemistry, thank you for making the time I spent with you incredibly fun and supportive.

Lastly, I want to give a huge thanks to my family and friends. Even if most of you had no idea of what I was talking about half the time, you always gave me love, support and encouragement during the months I spent working on this thesis. Without you I would not have made it this far and for that I am incredibly grateful.

Alva Nilsson, Gothenburg, June 2025

List of Acronyms

Below is the list of acronyms that have been used throughout this thesis listed in alphabetical order:

AMP	Antimicrobial peptide
AuNP	Gold nanoparticle
AuNR	Gold nanorod
BAI	Biomaterial-associated infection
BHI	Brain-heart infusion
CFU	Colony forming units
E. coli	*Escherichia coli*
EDC	1-(3-dimethylaminopropyl)-3-ethylcarbodiimide
LSPR	Localised surface plasmon resonance
MES	2-Morpholinoethanesulponic acid
MH	Mueller-Hinton
MHB	Mueller-Hinton broth
MIC	Minimum inhibitory concentration
MQ	Milli-Q
NHS	hydrochloride-N-hydroxysuccinimide
NIR	Near-infrared
OD	Optical density
PBS	Phosphate buffer saline
S. aureus	*Staphylococcus aureus*
SEM	Scanning electron microscopy
TSB	Tryptic soy broth

Contents

List of Figures

List of Tables

1

Introduction

The use of biomaterials has a long and extensive history spanning several millennia and various cultures [1]. A few early examples are dental implants, prosthetic limbs, and gold used to repair skull deformations. As science evolves, biomaterials can today be found in a vast array of medical devices such as prosthetic joints, urinary catheters and intravascular stents [2]. Biomaterial use in modern medicine allows us to ensure health, quality of life and maintenance of bodily functions. Utilisation of biomaterials is expected to increase in the foreseeable future as the global population ages due to reduced fertility rates and increased life expectancy, leading to age-related diseases becoming a more abundant problem [3]. A study published in 2018, encompassing 38 countries, predicts the use of hip implants alone to increase with 50% by the year 2050 [4].

A major concern regarding the use of biomaterials is the risk of patients acquiring biomaterial-associated infections (BAIs) [5]. These infections occur due to bacterial contamination of the biomaterial surface, e.g. during surgical implantation [2]. If the contamination is not eradicated by the immune system or antibiotic therapy, biofilm formation can occur and result in a chronic infection. Once a BAI is established it is difficult to treat due to the biofilm matrix shielding bacteria from the environment. Furthering the concern of BAIs is the increased occurrence of bacteria acquiring antimicrobial resistance (AMR) [6]. When bacteria develop resistance to antibiotics and antimicrobials, the resulting BAIs become even more difficult to prevent and treat than they already are.

The increase in biomaterial use, along with the increased risk of acquiring antibiotic resistant infections, leads to a need for new methods to prevent and effectively treat bacterial contamination on biomaterial surfaces. A method of preventing BAI development, that has gained increased interest in recent years, is the use of antibacterial surface modifications [7]. A promising surface modification aimed at eradicating bacteria is photothermal therapy [8]. When photothermal agents, such as gold nanorods (AuNRs), are exposed to light at their resonance frequency, they produce localised heat. This heat is used to damage and kill bacterial cells in the vicinity of the photothermal agent.

Another promising surface modification is the incorporation of antimicrobial peptides (AMPs) [7]. AMPs are broad-spectrum antibiotics that selectively target bacterial membranes of a wide variety of bacteria, including many resistant to conventional antibiotics [7, 9]. They are also less likely to contribute to antimicrobial

resistance as they target general, rather than specific, structures of bacterial membranes [10].

Combining photothermal therapy with AMPs could result in a biomaterial surface able to eradicate bacterial contamination by two different mechanisms. This increases the probability of preventing BAIs, as well as doing so despite, and without contributing to the prevalence, of AMR. It is even possible that the effects of the two treatments could work together in such a way that one modification increases the susceptibility of the bacteria to the other and vice versa.

1.1 Aim

The aim of this thesis was to evaluate the antibacterial activity of NIR irradiated AuNR functionalised glass surfaces in combination with AMPs, when assessed against *Staphylococcus aureus*. It was hypothesised that the heat damage to bacterial cells caused by irradiation of the AuNRs, and the bacterial membrane disruptive effect of the AMPs, could act synergistically.

2
Theory

The following chapter gives an overview of the theoretical background, laying the foundation for understanding the topic of this thesis. A general introduction to biomaterials, their applications as well as their importance and challenges in modern medicine, will be followed by a deep dive into a specific biomaterial surface modification. Thereafter, the bacterium employed in this thesis will be presented, and lastly, the different characterisation techniques used to evaluate antibacterial activity will be described.

2.1 Biomaterials

The term "biomaterial" has long been discussed and continuously redefined as the fields of material science and healthcare technology evolve [11]. A recent definition of the term biomaterial was decided upon at a consensus conference held in 2018 in Chengdu, China [12]. 53 biomaterials experts from 17 countries came to the consensus that a biomaterial should be defined as follows:

> "A material designed to take a form that can direct, through interactions with living systems, the course of any therapeutic or diagnostic procedure."

Biomaterials in medical devices encompass a wide variety of applications such as cardiovascular devices, joint replacements, and diagnostic tools [2]. The materials of which these medical devices are made can range widely from abiotic materials such as metals, ceramics, and polymers to biological materials such as devitalised blood vessels and xenobiotic heart valves.

2.1.1 Biomaterial-associated infections and antimicrobial resistance

As the incidences of biomaterial use in modern medicine increase, so does the concern for complications due to biomaterial-associated infections [2]. Biomaterial implants, such as joint replacement prosthetics, have an increased susceptibility to infection stemming from bacterial colonisation of the biomaterial surface. If the immune system, or preventions such as antibiotic therapy, cannot eradicate the bacterial contamination, biofilm formation can occur and result in a chronic BAI. The occurrences of BAIs in hip prosthetic joints range from 0.5-1% in hip and knee replacements to 5% in elbow and ankle replacements [2, 5]. Bacterial colonisation can occur during the surgical procedure, but there is an additional lifelong risk of

acquisition due to bacteremia and local skin infections [2]. Once a biofilm is formed, the bacteria produces, and becomes encased in, a polysaccharide matrix adhering to the surface. The bacteria encased within the matrix becomes less susceptible to antibiotic treatment and the host's own immune defense. These infections require surgical interventions and long-term antibiotic treatment, affecting the functional outcome of the implant, and in some cases resulting in complete removal. *S. aureus* is a bacteria commonly responsible for BAIs in most medical implants such as prosthetic joints, mechanical heart valves and urinary catheters, which makes it of special interest [13]. *S. aureus* is a highly virulent, Gram-positive cocci found colonising, for example, the skin and nasal cavity of about 30-50% of healthy adults [14]. It is a common pathogen causing pneumonia, wound infections, and abscesses when entering the body through damaged skin and mucosal barriers.

A further concern regarding BAIs is the increased occurrence of bacterial antimicrobial resistance (AMR). It has been estimated that a total of about 4.95 million deaths were associated with bacterial AMR in 2019, and that by 2050, AMR could lead to the deaths of 10 million people annually [6]. Bacteria can acquire resistance by genome mutations or exchange of resistant genetic sequences [15]. The more bacteria are exposed to antibiotics the higher the risk is of them developing resistance through mutations, limiting treatment options. Two pathogens were identified to be responsible for about half of all AMR related deaths in high-income countries, being *Staphylococcus aureus* and *Escherichia coli* [6]. Notably, *S. aureus* is, as previously mentioned, a common cause of BAIs. This further highlights the importance of research aimed at finding novel methods for treating and preventing BAIs.

As the incidences of BAIs increase and AMR becomes an ever-growing concern, there is an urgent need to develop biomaterials that can efficiently and rapidly eradicate or prevent bacterial contamination without relying on conventional antibiotics. One strategy that has gained interest in recent years is the use of antimicrobial surfaces [7]. Antimicrobial surface modifications primarily focus on preventing or combating bacterial colonisation through chemical or physical mechanisms. Surface modifications based on chemical mechanisms are, for example, anti-adhesive surfaces incorporating hydrogels and polymers that prevent bacterial attachment, and bactericidal surfaces that make use of biocides or photocatalytic particles. Physical mechanisms often focus on, but is not limited to, topographical modifications on the micro- and nanoscale that prevent bacterial adhesion.

2.2 Photothermal therapy utilising gold nanorods

A promising biomaterial surface modification based on physical mechanisms, other than topography, is the use of photothermal therapy, which is a technique in which a photothermal agent absorbs light and produces localised heat [8]. As photothermal agents are exposed to light of their resonance frequency, their electrons are excited. When the electrons subsequently decay to their ground state through nonradiative decay they emit excess energy as heat to the local surroundings. Gold nanoparticles (AuNPs) are useful as photothermal agents due to their efficient absorption of radi-

ation, which allows relatively low energy light to be absorbed. This phenomenon is attributed to noble metal nanoparticles, such as AuNPs, exhibiting localised surface plasmon resonance (LSPR). LSPR refers to a phenomenon in which light excites surface electrons in the conduction band in metallic nanostructures [16], leading to coherent plasmon oscillations in the electron cloud with a specific resonance frequency. This frequency depends on the physical attributes of the particles, such as shape and size. AuNP dimensions can be tuned to absorb light in a certain spectral region and produce heat as a result. Gold nanorods (AuNRs) are preferably used in applications such as biomaterial surface modifications, as they can be tuned to absorb light in the near infrared (NIR) spectrum which is minimally absorbed by tissue [17]. Due to the shape of AuNRs oscillations can occur in two directions, either in the transverse or the longitudinal direction. It is the longitudinal absorption band of AuNRs that can be tuned to the NIR region, by increasing the aspect ratio length divided by width. A study using AuNRs with the length/width ratio of 67 $\pm$ 7 nm and 18 $\pm$ 2 nm showed a longitudinal LSPR band of 808 nm, which is in the NIR region [18].

2.3 Antimicrobial peptides

Another interesting possibility for antimicrobial surface modifications is the incorporation of antimicrobial peptides (AMPs). AMPs are short sequences of amino acids, typically between 12-50 amino acids long, and predominantly carry a positive charge [19]. Practically all organisms produce AMPs through their immune systems, as they can act as broad-spectrum antimicrobials against both Gram-positive and Gram-negative bacteria, as well as fungi and parasites. Cationic AMPs are of particular interest for antibacterial applications, as their net positive charge causes them to favourably target bacterial membranes, which usually carries a net negative charge [10]. The cells of multicellular animals, on the other hand, carry no net charge leading to AMPs selectively targeting bacterial cells. The most well-known mode of action of AMPs is the disruption of cell membranes. Many AMPs have, however, also shown the ability to translocate into the interior of bacterial cells to target and disrupt intracellular processes [20]. Contrary to conventional antibiotics AMPs have been proven to induce resistance in bacteria to a considerably lesser extent [10]. This can be attributed to the fact that AMPs do not target a specific membrane structure, but the membrane itself and as such, the resistance development potential is lower. A bacteria fundamentally changing its membrane structure would most probably be a far too energy demanding process to undertake.

The AMPs used in this project were RRP9W4N and CC-RRP9W4N. The RRP9W4N is an AMP consisting of 13 amino acids in the sequence RRPRPRPRPWWWW, see Figure 1. It is cationic with a net charge of +6 at physiological pH and a molecular weight of 1930 g/mol. The RRP9W4N AMP has polar amino acids close to the N-terminus that are attracted to bacterial membranes. Nonpolar groups are found at the C-terminus, allowing the AMP to interact with the lipids in the membrane and exert an antibacterial effect. This AMP was chosen for the project as a previous study determined that the RRP9W4N AMP showed significant antibacterial

activity [21]. The same study showed that this AMP has a minimum inhibitory concentration, the concentration at which an antimicrobial agent can reduce bacterial growth by 80%, of 6-12 µM.

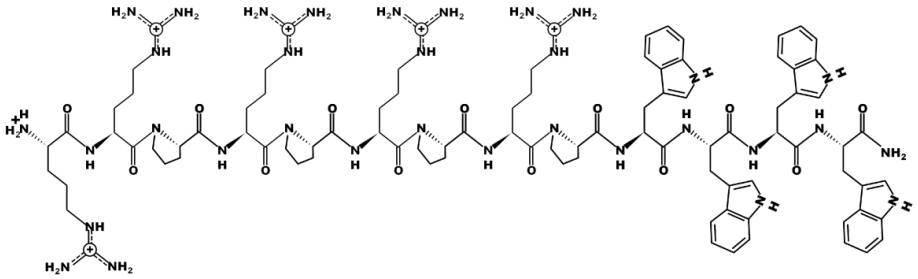

Figure 1: Chemical structure of the AMP RRP9W4N.

CC-RRP9W4N, see Figure 2, is a modified version of the previous AMP, where two cysteine groups are added to the N-terminus, which is also acetylated. It has the complete amino acid sequence CCRRPRPRPRPWWWW, with a net charge of +6 at physiological pH and a molecular weight of 2178 g/mol. The addition of cysteine groups allows the AMP to bind to AuNRs via thiol bonds. This is a proven concept for functionalising gold nanoparticles with biomolecules [22].

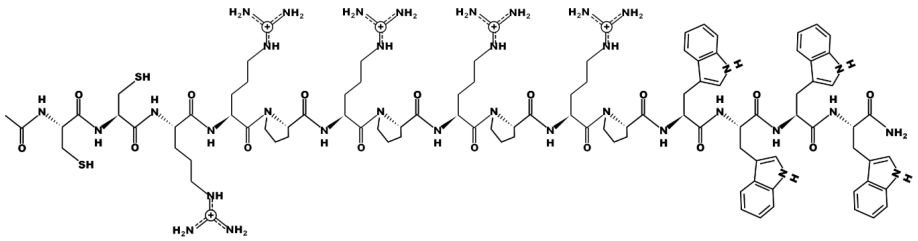

Figure 2: Chemical structure of the AMP CC-RRP9W4N.

3
Methods

This chapter will cover descriptions of characterisation techniques as well as the materials used during the experiments. Three experiments will be explained in detail: antibacterial susceptibility testing, an agar plate model, and fluorescence microscopy evaluation. All chemicals and growth media used during the experiments were acquired from Sigma-Aldrich Sweden AB, unless otherwise stated.

3.1 Preparation of bacterial suspension

All experiments were performed with the bacterium *Staphylococcus aureus* CCUG 10778. For long-term storage, the bacterial stock was stored at -80 °C. During the course of the experiments brain-heart infusion (BHI) agar plates were streaked with the stock solution of *S. aureus* and left to incubate overnight at 37 °C. Prepared plates were stored at 4 °C and used within one week, as prolonged storage leads to slowed growth rate.

To obtain bacterial suspensions used in the experiments, colonies of *S. aureus* were inoculated in tryptic soy broth (TSB) and incubated at 37 °C until the bacteria reached the middle of their logarithmic growth-phase. All concentration measurements of bacterial suspensions were performed with a Biowave WPA CO8000 Cell Density Meter, recording the optical density (OD) at 600 nm, unless otherwise stated. The bacterial suspension concentration is expressed as colony forming units per millilitre (CFU/ml), a CFU respresenting a single, viable bacterial cell able to form a colony on solid growth media.

3.2 Antibacterial activity evaluation

Three separate methods were used to evaluate the antibacterial properties of the surface modification comprised of AuNRs in combination with two different AMPs, RRP9W4N and CC-RRP9W4N, both acquired from GenScript. Antimicrobial susceptibility testing was performed to determine the minimum inhibitory concentration (MIC), the concentration at which an AMP was able to eradicate 80% or more of bacteria in a suspension. An agar plate model was used to determine the antibacterial properties by observing the number of colonies able to form under an antibacterial surface on solid growth media. Lastly, fluorescence microscopy was utilised to observe the antibacterial properties of the surfaces by how different treatments affected a monolayer of bacteria seeded onto the modified surfaces.

3.2.1 Antimicrobial susceptibility testing

The aim of an antimicrobial susceptibility test is to determine the susceptibility of a microorganism to an antimicrobial agent [23]. There are a variety of these tests, though the most commonly used is the MIC assay. A MIC assay can be performed in two ways, either as an agar dilution or as a broth dilution [24]. MIC assays performed in broth dilution should be executed with the growth media Mueller-Hinton broth (MHB), in which a concentration series of the antimicrobial agent to be studied is made and deposited into e.g. the wells of a 96-well microtiter plate. A bacterial suspension with the concentration of $5 \cdot 10^5$ colony forming units (CFU)/ml is then added to the wells and the plate is incubated for 16-20 hours depending on the bacterial strain used. The MIC is then determined as the lowest concentration of the antimicrobial agent which inhibits visible growth (turbidity) in the wells.

Following is a description of how antimicrobial susceptibility testing was performed in this thesis. One colony of *S. aureus* was inoculated in 4 ml TSB and incubated at 37 °C until an OD of 0.55-0.70 was measured, conferring a concentration of approximately 10^8 CFU/ml. The suspension was then diluted with MHB to a concentration of 10^6 CFU/ml. The MIC test was performed in a 96-well plate with 100 µl suspension in each utilised well, see Figure 3. Three wells were allocated to sterility control where pure MHB was added. Another three wells were allocated to growth control where 50 µl bacterial suspension was diluted with 50 µl MHB, resulting in a bacterial suspension with the concentration of $5 \cdot 10^5$ CFU/ml.

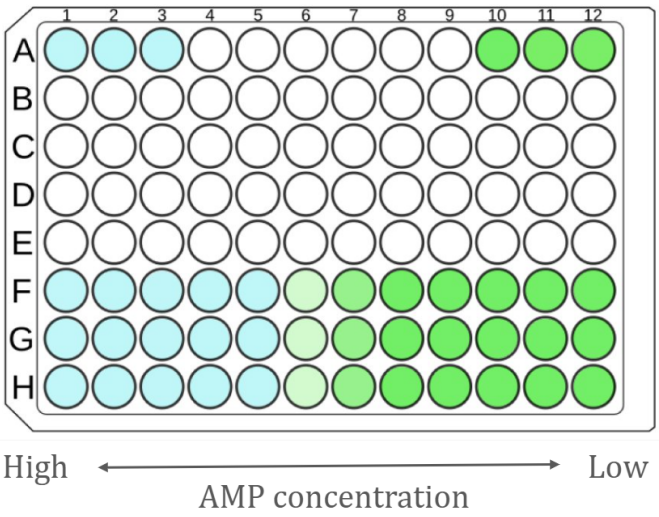

Figure 3: Illustration of a 96-well microtiter plate used for antibacterial susceptibility testing. The top three wells in blue are sterility control depicting pure MHB and the top three wells in green depict growth control inoculated with 10^8 CFU/ml of bacterial suspension in MHB. The three lower rows depict a serial dilution of AMPs ranging from high to low concentration inoculated with 10^8 CFU/ml of bacterial suspension in MHB.

Two different AMPs were evaluated, the RRP9W4N and the CC-RRP9W4N. To evaluate the antibacterial effect of the AMPs, a solution of AMPs dissolved in MHB underwent a 2-fold serial dilution to achieve a concentration series of wells containing 50 µl AMP suspension within the desired range. The concentration range differed between experiments, but was consistently within 200-0.0975 µM. Depending on the individual MIC test, up to three rows of 12 wells each were allocated to determine the OD of the AMP serial dilution by adding 50 ml MHB to the wells with AMP suspension. This was done to subtract the turbidity of the AMPs from the turbidity caused by the actual bacterial growth. In the three bottom rows of 12 wells each, 50 µl of bacterial suspension was added to the AMP dilution series resulting in a bacterial concentration of $5 \cdot 10^5$ CFU/ml, see Figure 3. The plate was incubated overnight at 37 °C and subsequently analysed in a Thermo Scientific Multiscan Go plate reader to record the OD at 600 nm in each well. The MIC was determined as the AMP concentration which resulted in an OD value 80% lower than that of the growth control wells.

3.2.2 Agar plate model

Agar is a hydrogel that is commonly used as a component in solid media for cultivating bacteria, e.g. in agar plates [25]. This thesis utilised an agar plate model developed to evaluate the antibacterial activity of surfaces [26]. In this model, surfaces are placed face down onto agar plates inoculated with bacteria, left to incubate overnight and the number of colonies formed under the surfaces are subsequently used for evaluation. The glass surfaces used in all experiments and for all sample groups in this thesis had a surface area of approximately 0.95 cm^2.

In some agar plate model experiments it was of interest to test for possible synergism of AuNRs in combination with AMPs. Synergism is a term commonly used in the context of describing effects of drug combinations [27]. At its core, however, it is a term to describe the combined effect of two treatments and can thus be used in other contexts such as biomaterial surface modifications. When two treatments are applied simultaneously, their combined effect can categorised as either synergistic, additive, or antagonistic [28]. An additive effect is observed when the combined effect of two treatments is equal to the sum of their separate effects, i.e. 1+1=2. A synergistic effect is observed when the combined effect is larger than the sum of separate effects, 1+1>2. Lastly, an antagonistic effect is observed when the combined effect is smaller than the sum of separate effects, 1+1<2. To determine whether the combination of AuNRs and AMPs showcased a synergistic, additive or antagonistic relationship, the Bliss independency model was used [27]. This model uses percentage inhibition Y_a and Y_b for treatment a and b, respectively, to calculate a predicted combined percentage inhibition $Y_{ab,P}$. This is done by the following equation:

$$Y_{ab,P} = Y_a + Y_b - Y_a Y_b \tag{1}$$

A relationship is then categorised based on if the observed combined percentage inhibition $Y_{ab,O}$ is larger, equal, or smaller than the prediction.

$$Y_{ab,O} = \begin{cases} > Y_{ab,P} & Synergistic \\ = Y_{ab,P} & Additive \\ < Y_{ab,P} & Antagonistic \end{cases} \quad (2)$$

As will be presented in the next chapter, a low antibacterial activity of the AMP CC-RRP9W4N was discovered during the antibacterial susceptibility testing. Focus was instead shifted to using the unmodified AMP RRP9W4N. Due to this shift another method for functionalisation had to be used. 1-(3-dimethylaminopropyl)-3-ethylcarbodiimide hydrochloride-N-hydroxysuccinimide (EDC/NHS) coupling is a common method for linking peptides to AuNPs [29]. In EDC/NHS coupling an EDC crosslinker is attached to a carboxylic acid, in this project being cysteine functionalised onto the AuNR [30]. NHS is then coupled to the carboxyl group, forming a stable NHS ester. Lastly NHS reacts with a primary amine, in this project being the amine group at the end of RRP9W4N, releasing the NHS and linking the AuNR to the AMP via a resulting amide bond.

The procedure of functionalising AuNRs with AMPs was not performed as part of this thesis, but will be presented for clarity. AuNR functionalised glass surfaces were sterilised in an UV/O_3 oven for 5 minutes to remove organic contaminants. The samples were then immersed in 1 mM of cysteine for approximately one hour and subsequently rinsed with Milli-Q (MQ) water. Next, the surfaces were immersed in EDC/NHS activation solution (1 mg/ml of EDC and NHS respectively, in 2-Morpholinoethanesulponic acid buffer at pH 5.5). Rinsing in MQ-water was repeated, followed by immersion in 200 µM RRP9W4N AMP solution for two hours. Lastly the surfaces were rinsed in MQ-water once more.

The agar plate model experiments performed were initialised in the same manner as the antimicrobial susceptibility tests, one colony of *S. aureus* was inoculated in 4 ml TSB, then incubated until an OD of 0.55-0.70 and a concentration of approximately 10^8 CFU/ml was reached. Two different setups of agar plate model experiments were performed.

In the first experimental setup, three sample groups of AuNR functionalised glass surfaces were used. Initially nine AuNR functionalised glass samples were sterilised in a UV/O_3 oven for 5 minutes to remove any organic contamination left on the surfaces during the synthesis protocol. The first group of samples consisted of AuNR surfaces to be irradiated with NIR light, the second of AuNR surfaces additionally functionalised with RRP9W4N AMPs and the third of AuNR surfaces functionalised with RRP9W4N AMPs to be irradiated with NIR light. The AMP functionalisation was not performed as part of this project, the surfaces had been previously functionalised with AMPs using cysteine and EDC/NHS as described earlier. The samples were then washed three times by placing them in the wells of a 24-well plate in 1 ml sterile filtered MQ-water. An illustrative explanation of the different sample groups can be seen in Figure 4.

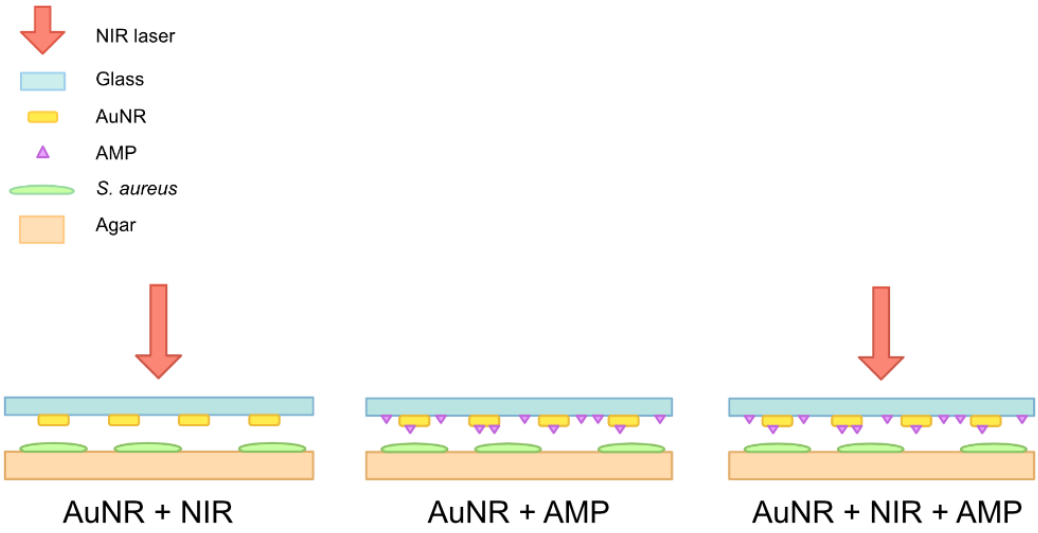

Figure 4: Illustration of sample groups in the first agar plate model experiment.

The 10^8 CFU/ml bacterial suspension was diluted with phosphate buffer saline (PBS) resulting in a bacterial suspension with the concentration $7 \cdot 10^4$ CFU/ml. Cotton swabs were dipped in the suspension for 5 seconds and streaked onto MH-agar plates. The samples were then placed with the AuNR functionalised side down toward the agar/bacteria. The sample groups AuNR + NIR and AuNR + NIR + AMP were irradiated with 808 nm NIR light at an effect of 16 W/cm^2 for 30 seconds. After irradiation, the plates were incubated at 37 °C overnight and the next day the colonies formed under each surface were photographed and counted to evaluate the antibacterial effect of the different modifications. Colonies growing in the outer 1 mm of the sample surfaces were not included, to avoid growth affected by the proximity to the surface edges to influence the results.

The second experimental setup differed from the first by the RRP9W4N AMPs being added to the bacterial suspension instead of being functionalised onto the AuNRs. Six glass samples and six AuNR samples were cleaned in a UV/O_3 oven for 5 minutes. Four different sample groups were used. The first and second groups were glass surfaces on bacterial suspension and bacterial AMP suspension respectively. The third and fourth groups were AuNR glass surfaces on bacterial suspension and bacterial AMP suspension respectively, both to be irradiated with NIR light. Figure 5 illustrates the different sample groups.

This experimental setup was used for assessing two AMP concentrations, 6.25 µM and 3.125 µM. For simplicity, the following description will only refer to the 3.125 µM procedure as all other steps were identical. Initially, the 10^8 CFU/ml bacterial suspension was diluted with PBS resulting in a $7 \cdot 10^4$ CFU/ml suspension with bacteria. Another bacterial suspension was prepared in the same manner, but was additionally supplemented with AMPs, resulting in a $7 \cdot 10^4$ CFU/ml and 3.125 µM

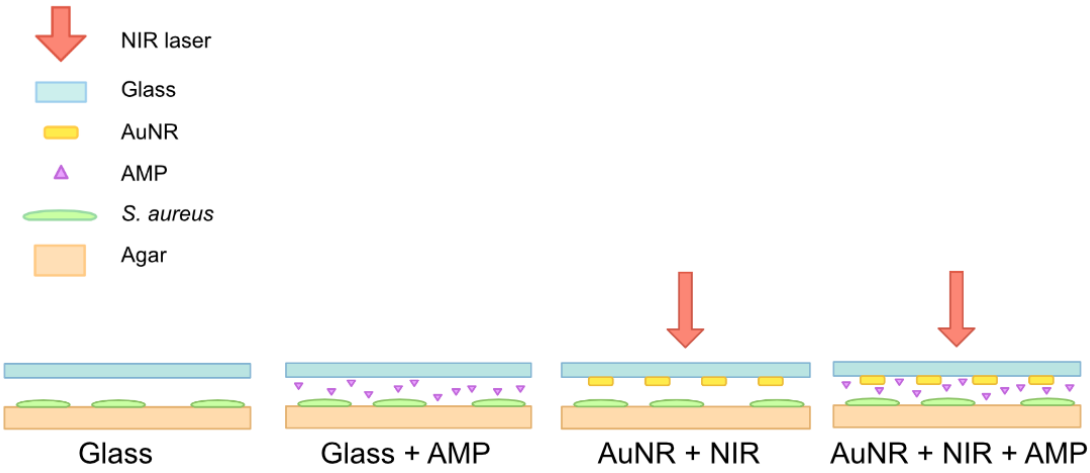

Figure 5: Illustration of sample groups in the second agar plate model experiment.

bacterial AMP suspension. Subsequently, MH-agar plates were streaked with the prepared suspensions by dipping cotton swabs in the suspensions for 5 seconds. This resulted in two MH-agar plates streaked with $7 \cdot 10^4$ CFU/ml bacterial suspension and two plates streaked with $7 \cdot 10^4$ CFU/ml and 3.125 µM bacterial AMP suspension. The samples were then placed with the modification facing down towards the agar. Three glass and three AuNR surfaces were placed on two agar plates streaked with the bacterial suspension. The remaining three glass and three AuNR samples were placed on two agar plates streaked with bacterial AMP solution. Afterwards the plates were incubated at 37 °C overnight. The following day the plates were photographed and the colonies formed under the sample surfaces were counted to evaluate the antibacterial effect. Colonies originating from within 1 mm of the surface edge were excluded for the same reasons as stated in the previous setup.

3.2.3 Fluorescence microscopy

Fluorescence microscopy is a type of microscopy that utilises fluorescent compounds, called fluorophores, to better visualize objects of interest against a black background [31]. Fluorophores are molecules that, when exposed to exciting light at their absorption wavelength, shortly thereafter emit light with a shorter wavelength. Filtering out the exciting wavelength when observing a sample through a fluorescence microscope leaves only the emitted wavelength, and thus only the fluorophores remain visible. This type of microscopy is often used in biology when examining bacterial viability, i.e. if the bacteria are alive or dead [32]. Bacterial viability tests, such as the LIVE/DEAD® BacLight™ kit, make use of two fluorophores. The first fluorophore, called PI, produces a red fluorescent signal when bound to DNA and can only enter dead cells with disrupted membranes. The second fluorophore, SYTO9, produces a green fluorescent signal and enters both live and dead cells, but is displaced from dead cells when PI is present. With both fluorophores present SYTO9 stains only live cells and emits a green signal, while PI stains only dead cell and

emits a red signal. By this principle it can be determined what amount of cells are live (appearing green) and what amount of cells are dead (appearing red), when observing bacteria through a fluorescence microscope. Fluorescence microscopy images taken of all experiments were analysed using "Fiji", a distribution of the open-source software "ImageJ" [33]. In this thesis Fiji was used to determine the percentage of dead cells in a fluorescence microscopy micrograph based on how many cells in total was present in the sample. This was done in order to evaluate the antibacterial activity of the surface modifications.

The fluorescence microscopy experiments were performed using two different setups. The first experiment began by rinsing three glass samples with 95% ethanol, followed by rinsing with MQ-water and drying with nitrogen gas. The three glass samples, along with 6 AuNR functionalised glass samples, were then cleaned in a UV/O_3 oven for 5 minutes. Bacterial suspension preparation began by centrifugation, in a MPW-150R centrifuge, of 4 ml of 10^8 CFU/ml bacterial suspension at 4000g for 5 minutes in order to harvest the cells. After centrifugation, 3 ml of the supernatant was removed and the pellet was then resuspended by adding 4.5 ml of PBS. The resulting 5.5 ml suspension had a concentration of approximately $0.73 \cdot 10^8$ CFU/ml. All samples were placed in 24-well microtiter plate wells and inoculated by adding 0.6 ml $0.73 \cdot 10^8$ CFU/ml bacterial suspension diluted with 0.4 ml PBS. The dilution resulted in a $0.44 \cdot 10^8$ bacterial suspension and the microtiter plate was then incubated at 37 °C for 30 minutes. Following the incubation the samples were washed by moving them to new wells filled with 1 ml PBS, two times. The AuNR samples were thereafter irradiated with NIR light at an irradiance of 14 W/cm^2 for 30 seconds. The three glass samples and three of the AuNR samples were subsequently moved to new wells with 1 ml of 3.125 µM RRP9W4N AMP suspension and allowed to incubate at room temperature for one hour. During this time live/dead stain was prepared by adding 2.25 µl of solution A (1.6 mM SYTO9, 1.67 mM PI) and 0.75 µl of solution B (1.67 mM SYTO9, 18.3 mM PI) to 1 ml 0.85 wt% NaCl. The live/dead stain was produced with a LIVE/DEAD® BacLight™ Bacterial Viability Kit acquired from Thermo Fisher Scientific Inc. After the incubation in the AMP suspension all samples were placed on microscopy slides, 10 µl of live/dead stain was added and the samples were brought to be evaluated by fluorescence microscopy. An illustration depicting the different sample groups can be seen in Figure 6.

The second experimental setup began by cleaning two glass samples and four AuNR functionalised glass samples in a UV/O_3 oven for 5 minutes. Following that, 8 ml of 10^8 CFU/ml bacterial suspension was centrifuged at 4000g for 5 minutes and 7 ml of the supernatant was removed. The pellet was then resuspended by adding 4.5 ml PBS, resulting in a bacterial suspension of approximately $1.45 \cdot 10^8$ CFU/ml. All samples were placed in a 24-well microtiter plate and inoculated with 0.6 ml of the previously mentioned bacterial suspension diluted with 0.4 ml PBS, resulting in a 0.44 10^8 CFU/ml bacterial suspension. The plate was then incubated for 30 minutes at 37 °C, followed by twice washing the samples by moving them to new wells with 1 ml PBS. Two of the AuNR samples were moved to additional wells of 1 ml PBS, while the two glass samples and the two remaining AuNR samples were moved to

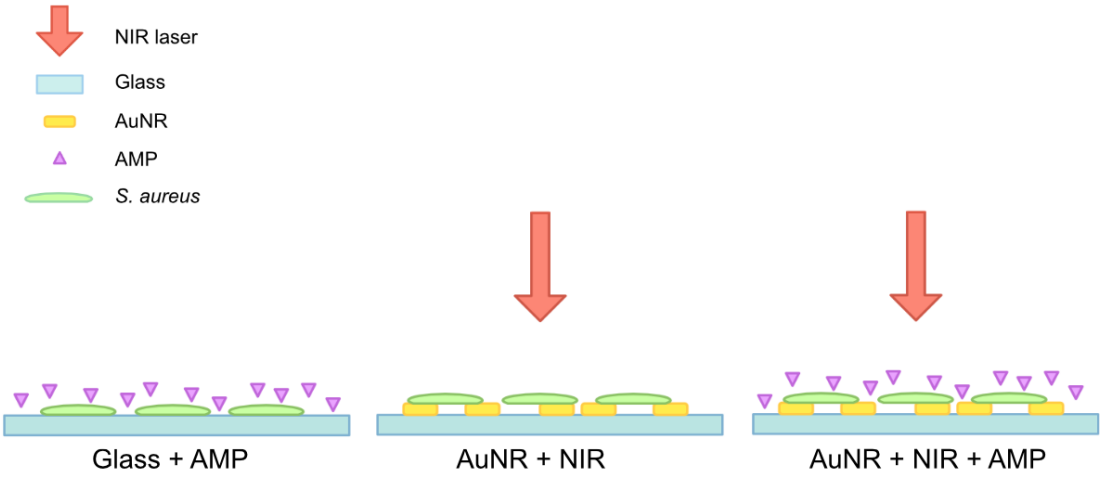

Figure 6: Illustration of sample groups in the fluorescence microscopy experiments.

wells filled with 1 ml of 6.25 µM RRP9W4N AMP suspension. The incubation in the AMP suspension took place in room temperature for 30 minutes. After the 30 minutes had passed, all the AuNR samples were irradiated with NIR light at an effect of 16 W/cm^2 for 30 seconds. Thereafter, the samples were incubated for an additional 30 minutes. During this time live/dead stain was prepared in the same manner as described in the previous experimental setup. Lastly, all the samples were placed on microscopy slides, 10 µl of live/dead stain was added and the samples were brought to the fluorescence microscope for evaluation. The different sample groups are illustrated in Figure 6.

3.3 Statistical analysis

Origin Pro is a data analysis and graphing software that was used for graph making and to perform statistical analyses in this thesis, specifically the 2023 version was used [34]. All sample groups in an experiment were tested against each other to determine whether there were any significant differences between them. When comparing two samples to each other it is appropriate to use a t-test [35]. A t-test is used to analyse any significant differences in mean values of two samples when the data is, or can be assumed to be, normally distributed. Since all sample groups were statistically independent, i.e. the results of one sample group were not influenced by the results of another, a two-sample t-test was used.

4

Results and discussion

In this chapter all results will be presented, interpreted and discussed. Firstly, characterisation of the AuNR surfaces will be presented. The next section will include results from the antibacterial susceptibility testing performed on the two different AMPs. Next, agar plate model experiments will be presented encompassing three separate sets with differing experimental conditions. Furthermore, two different fluorescence microscopy experiments will be presented and lastly the future perspective of how this research can move forward will be discussed.

4.1 Gold nanorod surfaces

Preparation of glass surfaces functionalised with AuNRs was not performed as part of this thesis, and neither was the characterisation of the surfaces. The results from the characterisation of the provided surfaces will however be presented here as the surfaces are an integral part of the whole project. The distribution of AuNRs on the glass surface is presented as a scanning electron microscopy (SEM) micrograph in Figure 7A and an absorption spectrum of the sample is presented in Figure 7B.

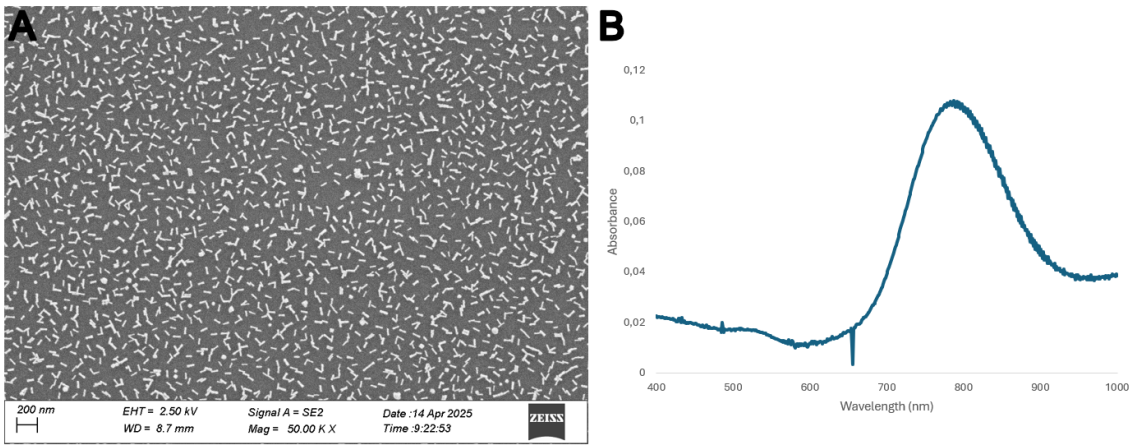

Figure 7: (A) SEM micrograph of AuNR functionalised glass and (B) absorption spectrum of AuNR functionalised glass in air.

As can be seen in Figure 7A the AuNR particles are indeed attached to the glass surface and in a sufficiently well dispersed manner. At ocular inspection the particles

cover approximately 10-15% of the surface, enough for a single cell of *S. aureus* in contact with any part of the surface to also be in contact with AuNRs. There are no large clusters of particles, meaning the majority of particles will have preserved localised surface plasmon properties. This preservation is evident when looking at Figure 7B. The longitudinal peak lies at 787 nm, this value is however for absorption in air. If the characterised sample had been in an aqueous solution, which they are when they are irradiated in the experiments, the peak would red-shift to lie somewhere around 808 nm. The absorption spectrum confirms that the plasmon resonance of the particles is conserved as it shows the characteristic transverse and longitudinal peaks at the appropriate wavelengths.

4.2 Antimicrobial susceptibility testing

In total eight antibacterial susceptibility tests were performed to evaluate the antibacterial activity of the AMPs CC-RRP9W4N and RRP9W4N. Initially, the CC-RRP9W4 was tested at three separate occasions, as it was intended to be the AMP functionalised onto the AuNRs due to the addition of cysteines able to form thiol bonds to gold. After the initial three tests, it was decided that the focus should instead be shifted to the RRP9W4N AMP for reasons that will become evident in the upcoming discussion of the results. The RRP9W4N AMP underwent five rounds of tests, and the results of all eight tests are presented in Table 1.

Table 1: Antibacterial activity of two AMPs, measured by their MIC in µM when assessed against the bacterium *S. aureus*.

AMP	**MIC (µM)**	**Number of replicates**
CC-RRP9W4N	100-200	3
RRP9W4N	25-50	5

As can be seen, the MIC for the CC-RRP9W4N AMP is between 100 and 200 µM. Such a high MIC renders the CC-RRP9W4N unsuitable for use in clinical applications, since unreasonable high dosages would be needed to achieve antibacterial activity *in vivo*. For this reason focus was shifted to the AMP RRP9W4N, which has a known MIC of between 6 and 12 µM. The known antibacterial activity of RRP9W4N was not successfully replicated during this thesis, instead a MIC of 25-50 µM was observed. Two tests indicated a MIC of 25 µM while three tests indicated a MIC of 50 µM, this range is about four times higher than the actual MIC range for the RRP9W4N. This discrepancy can possibly be explained by experimental errors, such as errors during the preparation of the dilution series, errors due or incorrect pipetting and the lack of uniform turbidity in wells. An additional possibility that could be responsible for the discrepancy is that the bacterial suspension was not used within an appropriate time frame after measuring its OD. This would lead to MIC values appearing higher than they actually are, as a higher concentration of bacteria was present than the standard suggests using. Regarding the difference in MIC values between the two AMPs, it is interesting to note that the only differences between them are the addition of two cysteine groups at the N-terminus of

CC-RRP9W4N, as well as the N-terminus being acetylated. That such a small modification had such a large effect on the antibacterial properties was not anticipated, and showcases how much AMP functionality is related to changes in composition. As presented in the theory chapter the antibacterial activity of AMPs are related to their composition. It is possible that the membrane disruptive effect of the AMP significantly decreased by the changes in properties such as mass, isoelectric point and hydrophobicity caused by the additional cysteine groups.

The shift to working with the RRP9W4N led to the planned functionalisation of AMPs onto the AuNRs having to be reworked. The original idea was that the cysteine groups on the CC-RRP9W4N would be used to functionalise the AuNRs with the AMPS, as described in the method section. Without the cysteine present in the RRP9W4N, new methods to perform the functionalisation using EDC/NHS coupling were investigated separate from the project and tested in one of the following agar plate model experiments.

4.3 Agar plate model

Two different experimental setups were used during the agar plate model experiments. The first setup was tested once, and the second setup was performed twice using differing experimental conditions.

The first setup was used once with three replicates for each of the sample groups, AuNR + AMP, AuNR + NIR and AuNR + NIR + AMP. Here, the AuNRs were intially functionalised with cysteine, and RRP9W4N AMPs were thereafter coupled to the cysteine via EDC/NHS coupling, resulting in AMP functionalised AuNRs. For detailed description and illustration of the groups, see the Method chapter. A NIR laser irradiance of 16 W/cm^2 was used to irradiate the latter two sample groups. The aim of this experiment was to assess whether this form of functionalisation and applied laser effect was effective. The results of this experiment can be seen in Figure 8.

Due to the fact that this experiment unintentionally lacked a proper control group, which should have been simply AuNR surfaces, it is hard to determine what the actual effect of the treatments were. As can be seen in Figure 8, the statistical analysis showed no significant difference between the tested sample groups. The large error bars show a very high deviation of results within the sample groups. This can be attributed the small sample size, but is most likely explained by a problem with the streaking method used to seed the agar plates that was discovered during the experiments. For an unknown reason, the first plate streaked from each suspension exhibited a significantly higher colony density than those streaked later, as can be seen in Figure 15 in Appendix 1. This finding led to alterations in the protocol of subsequent experiments in which the first cotton swab dipped in the bacterial suspension was discarded. As can be seen in Figure 16 in Appendix 1, this action led to a more uniform distribution of colony density in later experiments.

The lack of a control group made it hard to draw any clear conclusions whether the

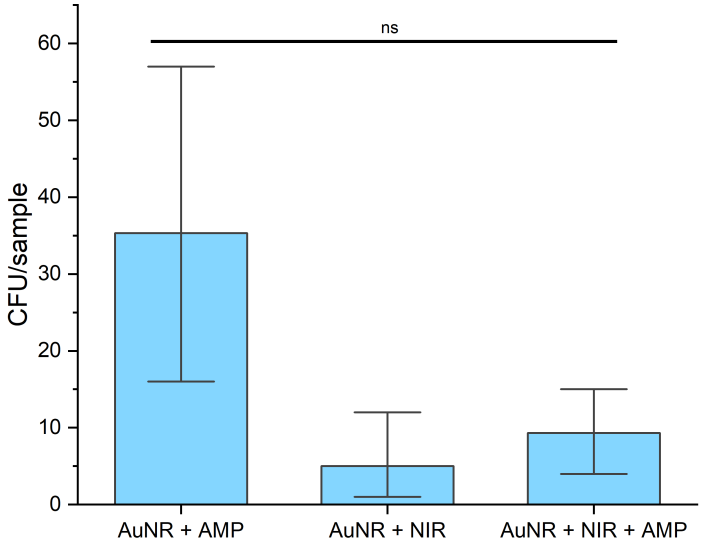

Figure 8: Results from antibacterial activity evaluation with the agar plate model using a $7 \cdot 10^4$ CFU/ml bacterial suspension, RRP9W4N AMP functionalised AuNRs, and 16 W/cm^2 NIR irradiation for 30 seconds. Results are recorded in CFU/sample. Bars represent mean value, n=3, and error bars represent standard deviation. Statistical difference is visualised by a thick line, indicating all combinations of groups below having the same significance level. Significance level (ns) no significance.

AMP functionalisation had any effect on bacterial growth. However, when compared to the overall growth on the plates outside of the samples, no major differences were observed. It was thus determined that no clear, or at least not significant enough, antibacterial activity of the AMP functionalisation was observed in this experiment. The cause of this was most likely problems with the functionalisation of AMPs onto the AuNRs itself. Figure 13 and 14 in Appendix 1 provide absorption spectra of AuNR surfaces before and after the initial cysteine functionalisation. After functionalisation the spectra almost completely lacks the characteristic transverse and longitudinal peaks, meaning little light was absorbed by the surfaces. The lack of absorption indicates a lack of AuNRs, and it can thus be concluded that the functionalisation causes the AuNRs to detach from the glass surface. This is likely observed due to the immersion in cysteine that occurs before the EDC/NHS coupling. While the AuNRs are attached to the glass surface via electrostatic forces, the cysteines attach through stronger thiol bonds to the gold. When cysteines bind to the AuNRs, their carboxyl groups cause the whole nanoparticles to gain a negative charge. Since the glass surface is negative as well, the AuNRs will be repelled and detach from the surface. Regarding the NIR laser irradiation, which was applied

in the AuNR + NIR and AuNR + NIR + AMP samples, a clear effect could be observed. Ocular observations between the surrounding bacterial density and the density of irradiated samples showed enough of a difference to conclude that a laser intensity of 16 W/cm^2 for 30 seconds was sufficient to apply in further experiments.

In the second experimental setup, focus was shited to evaluating antibacterial activity of AuNR surfaces in the presence of the AMP RRP9W4N. Instead of being functionalised onto the AuNRs, the AMPs were added to the bacterial suspension before streaking it onto the agar plates. The aim of these experiments was to investigate whether any synergism could be observed between the photothermal therapy and the antibacterial effect of AMPs. The first experiment performed with this setup consisted of the four sample groups Glass, Glass + AMP, AuNR + NIR, and AuNR + NIR + AMP. There were three samples in each group and the experiment was repeated once. The concentration of AMP in the bacterial suspension was 6.25 µM, which is in the lower MIC range. A NIR laser effect of 16 W/cm^2 for 30 seconds was used when irradiating photothermal therapy samples. The results of this experiment can be seen in Figure 9.

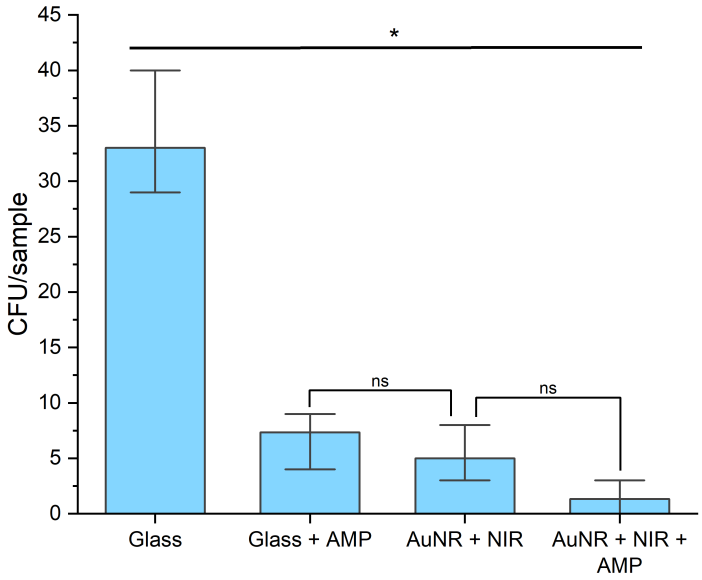

Figure 9: Results from antibacterial activity evaluation with the agar plate model using a $7 \cdot 10^4$ CFU/ml and 6.25 µM RRP9W4N bacterial AMP suspension, and 16 W/cm^2 NIR irradiation for 30 seconds. Results are recorded in CFU/sample. Bars represent mean value, n=3, and error bars represent standard deviation. Statistical difference is visualised by a thick line, indicating all combinations of groups below having the same significance level. Brackets are exceptions indicating significance levels between specific groups. Significance level (*) $p<0.05$, (ns) no significance.

As can be seen in Figure 9, this experiment shows significant differences with a 95% certainty between the control group Glass and all the other sample groups. This proves that an antibacterial activity was observed for all treatments. There was a significant difference between the groups Glass + AMP and AuNR + NIR + AMP. Since no significant difference was found between the AuNR + NIR group and the two other antibacterial treatments, the relationship between the photothermal treatment and the effect of the AMPs could not be definitely determined. To potentially better distinguish differences between the sample groups, a lower AMP concentration was utilised in the upcoming experiments.

The last agar plate experiment performed had the same four sample groups as the previous experiment, with 3 samples per group, and was repeated three times. The laser parameter was kept unchanged, but the concentration of RRP9W4N AMP was lowered to 3.125 µM, just below the MIC. These experimental conditions resulted in a significant difference being observed between all samples with at least 95% certainty, as seen in Figure 10.

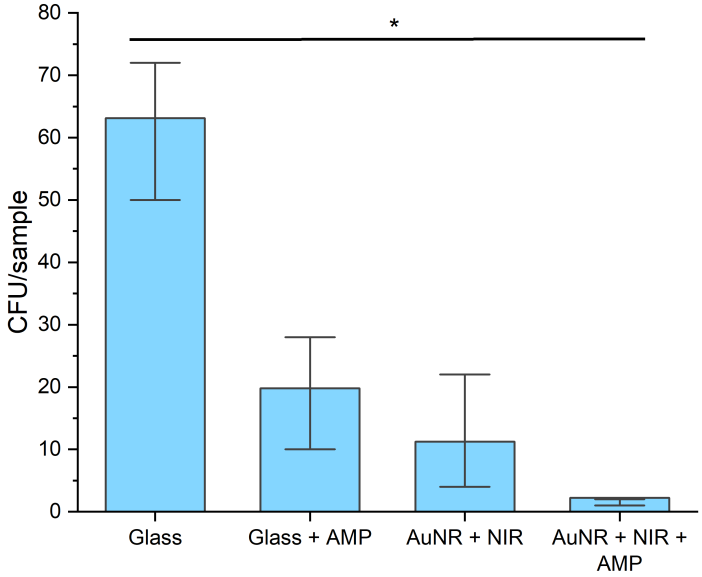

Figure 10: Results from antibacterial activity evaluation with the agar plate model using a $7 \cdot 10^4$ CFU/ml and 3.125 µM RRP9W4N bacterial AMP suspension, and 16 W/cm^2 NIR irradiation for 30 seconds. Results are recorded in CFU/sample. Bars represent mean value, n=9, and error bars represent standard deviation. Statistical difference is visualised by a thick line, indicating all combinations of groups below having the same significance level. Significance level (*) $p<0.05$.

Antibacterial activity is clearly expressed by all groups, the Glass + AMP and AuNR + NIR group killed about 69% and 82% of the bacterial population respec-

tively. The strongest antibacterial activity was however attributed to the AuNR + NIR + AMP group which killed about 96% of the present bacteria, which was expected as the two treatments were combined. To evaluate if any synergistic relationship between treatments existed, the Bliss independence model was used to calculate the predicted combined percentage inhibition $Y_{ab,P}$ of AuNRs and AMPs if they showed an additive relationship, see Equation 1. When the model was implemented, $Y_{ab,P}$ was calculated to be approximately 94%. The actual effect $Y_{ab,O}$ was, as mentioned, about 96%. As $Y_{ab,O}$ was higher than $Y_{ab,P}$, the effect was technically defined as synergistic using the Bliss independence model, see Equation 2. Although the difference was very small, the result alludes to synergism. It is possible that a more significant synergistic relationship could be determined if the sample sizes were increased. It could also be that AMPs properly functionalised onto an AuNR surface shows greater synergism, or that different experimental conditions are required. To conclude, the results show an increased antibacterial activity when photothermal therapy from NIR irradiated AuNRs on surfaces is combined with AMPs. A slight synergistic relationship is observed, but more research is needed to determine whether the synergism is significant.

4.4 Fluorescence microscopy

Results from two experiments evaluating the antibacterial activity of the three sample groups Glass + AMP, AuNR + AMP and AuNR + NIR + AMP will be presented. These experiments focused on AuNR surfaces immersed in a RRP9W4N AMP suspension after bacteria had attached, rather than utilising functionalised AMPs. The aim of this experiment was to study the antibacterial effect of photothermal therapy and antibiotic treatment with AMPs at a single-cell level rather than at a CFU level. Samples were stained with a LIVE/DEAD® BacLight™ kit to visualise cell viability. Results were recorded in % dead bacteria. To calculate the value % dead bacteria, the amount of dead bacteria in a micrograph were divided by the total amount of bacteria present in the same micrograph using image analysis.

In the first experiment samples were incubated in an AMP concentration of 3.125 µM for one hour after bacterial inoculation and 14 W/cm^2 NIR irradiation for 30 seconds. The results after staining and image analysis, along with visualisation of statistical differences, can be seen in Figure 11. Examples of images used for evaluation of the different groups can be found in Figure 17 in Appendix 1. The sample groups Glass + AMP, AuNR + NIR and AuNR + NIR + AMP were shown to kill about 5.2%, 1.6% and 2.8% of the bacteria present on a sample, respectively. A significant difference was observed between all sample groups. As is apparent from these results the NIR irradiation had little to no antibacterial activity, and could thus function as a form of control group. The AMPs however did show an antibacterial effect, the effect was slight but noticeable and statistically significant. Surprisingly, the combination of AuNRs and AMPs showed an antibacterial effect between the two other samples. It appears as though the presence of AuNRs inhibited the antibacterial activity of the AMPs. This should not be the case, and with the small sample sizes and lack of repeats this result can be questioned. It is

possible that the inhibition is due to other factors such as errors made during the experiment, but further experiments were needed to explore this.

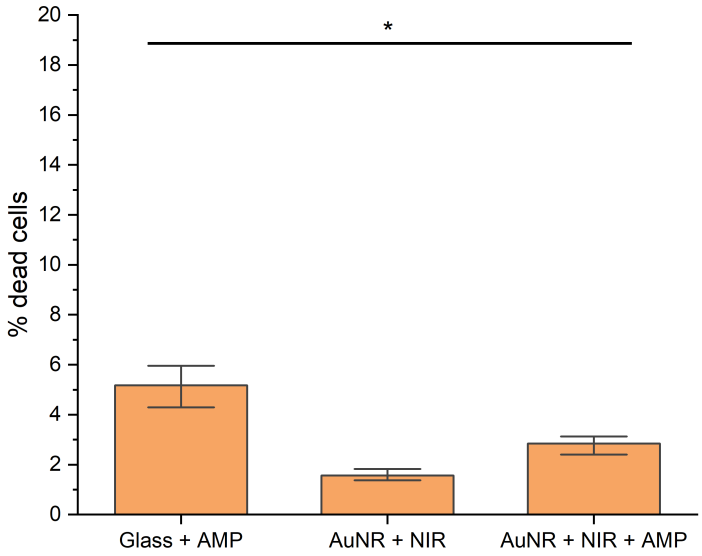

Figure 11: Results from antibacterial activity evaluation of sample groups when using fluorescence microscopy. Results are recorded as % dead bacteria of all bacteria present on a sample when 3.125 µM RRP9W4N AMP suspension and 14 W/cm^2 NIR irradiation for 30 seconds was used. Bars represent the mean value, n=3, error bars represent the standard deviation. Statistical difference is visualised by a thick line, indicating all combinations of sample groups below having the same significance level, (*) $p<0.05$.

The next fluorescence microscopy experiment performed differed from the first in three aspects. Firstly, the concentration of the AMP suspension was adjusted to 6.25 µM to hopefully increase the antibacterial effect. Secondly, the NIR laser effect was increased to 16 W/cm^2, as had proven to be effective in previous agar plate experiments. Lastly, the AuNR surfaces were incubated in AMP suspension 30 minutes before NIR irradiation and 30 additional minutes after. This method was used to maximise the combined antibacterial effect of AuNRs and AMPs, as the exact bactericidal mechanisms of tthe RRP9W4N AMPs are not known. It was speculated that the AMPs may weaken the bacterial membranes during the first 30 minutes, leading to the cells becoming more susceptive to the subsequent photothermal therapy. Further incubation in AMP suspension for another 30 minutes could potentially kill of bacteria that had been damaged due to heat exposure. The results from this experiment can be see in Figure 12, and examples of images used for evaluation of the different groups can be found in Figure 18 in Appendix 1.

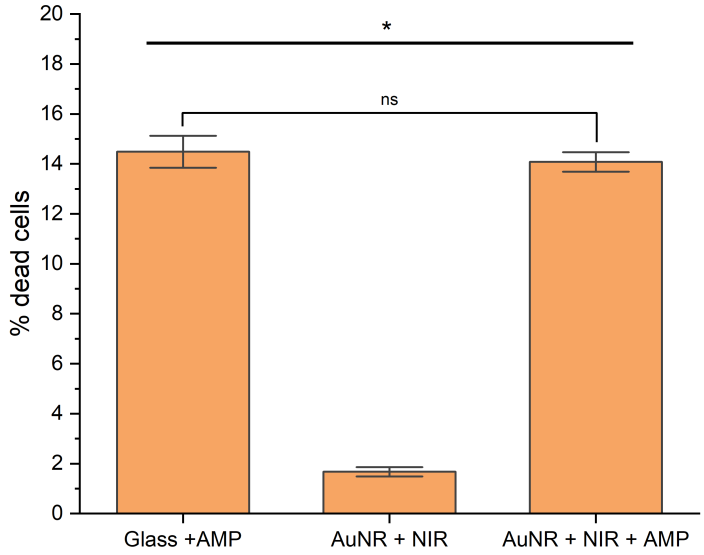

Figure 12: Results from antibacterial activity evaluation of sample groups when using fluorescence microscopy. Results are recorded as % dead bacteria of all bacteria present on a sample when 6.25 µM RRP9W4N AMP suspension and 16 W/cm^2 NIR irradiation for 30 seconds was used. Bars represent the mean value, n=2, error bars represent the standard deviation. Statistical difference is visualised by a thick line, indicating all combinations of sample groups below having the same significance level, (*) $p<0.05$, (ns) no significance.

The Glass + AMP, AuNR + NIR and AuNR + NIR + AMP sample groups were, in this experiment, able to kill 14.5%, 1.7% and 14.1% of the bacteria present on a sample, respectively. In this experiment, both the Glass + AMP and the AuNR + NIR + AMP groups showed a significant difference when compared with the AuNR + NIR group, with a certainty of at least 95%. However, the two groups did not show any significant difference when compared to each other. As the result from the AuNR + NIR group was very similar to that of the same group in the previous experiment, it can be concluded that the irradiation was inefficient at an effect of 16 W/cm^2 as well. While 16 W/cm^2 proved to be sufficient in the agar plate experiments, it is likely that the heat generated by samples submerged in liquid dissipated into said liquid before any thermal damage could be inflicted on the bacteria. In this experimental setup it is impossible to remove all liquid from the samples as it would dry them out, leading to skewed results as cells will start to die when exposed to open air. Minimising the amount of liquid also comes with the drawback of possibly boiling the cells as the liquid heats up. The setup could possibly be changed to circumvent this problem by switching to NIR irradiation on agar plates and removing the samples for staining afterwards.

When comparing the antibacterial activity of the groups Glass + AMP and AuNR + NIR + AMP, it can clearly be seen that they were very similar, unlike the previous experiment. There is no evidence of the AuNRs inhibiting the AMPs activity, in contrast to the first fluorescence microscopy experiment. Since no other evidence of an inhibitory effect was found in other experiments performed, it can be assumed that the effect in the previous experiment was due to experimental errors.

To conclude the results from the fluorescence microscopy experiments, the NIR laser had no effect when applied at 16 W/cm^2 in this experimental setup, most probably due to heat dissipation. Antibacterial activity could however be observed when samples were incubated in AMP suspension as low as 3.125 µM.

4.5 Future perspective

A major finding made during this thesis was the unsuitability of the AMP CC-RRP9W4N as an antibacterial agent when evaluated by antimicrobial susceptibility testing. The decrease in antibacterial activity was somewhat unexpected when only two amino acids were added to a structure with known antibacterial activity. Future research in finding a method to successfully functionalise AMPs to AuNRs needs to take into account that even small changes in AMP structure can have a significant effect on antibacterial activity.

Indications of synergism were found in agar plate experiments when RRP9W4N AMPs were added to the bacterial suspension. This is something that is worth exploring further by repeating experiments using more samples to explore whether the synergistic effect can be proven statistically significant. Once a proper functionalisation method to attach AMPs to the AuNRs is developed, it will also be worthwhile to explore possible synergistic effects when there are more interactions between the two treatments, and they are in closer proximity to each other.

Further steps towards more clinically relevant setups are something to aim for in future research. Steps towards this would be to test the surface modifications with a wider range of bacteria common in BAIs. It will also be important to branch into testing on biofilms to see if the combination of photothermal therapy and AMPs can act as a treatment of established BAIs rather than to prevent the infections.

5
Conclusion

The aim of this thesis was initially to evaluate the antibacterial activity of AuNRs functionalised with CC-RRP9W4N AMPs. In the early stages of the project it was discovered that this AMP did not perform well in antibacterial susceptibility tests, leading to shifting focus towards the RRP9W4N AMP with known antibacterial activity. An alternative functionalisation method was evaluated in an agar plate model experiment, but was ultimately deemed unsuccessful due to the method causing the AuNRs to detach from the glass surfaces. Further experiments were focused on antibacterial activity of AuNRs in combination with RRP9W4N AMPs in suspension, rather than functionalisation of AMPs onto the AuNRs.

Results from the agar plate model experiments showed significant antibacterial activity for both the photothermal therapy and RRP9W4N AMPs as well as their combination. A NIR laser effect of 16 W/cm^2 and concentration 6.25 µM were determined to be appropriate experimental conditions in this setup. In addition a slight synergistic effect was observed when the two treatments were combined, which would be interesting to explore further in the future. Fluorescent microscopy proved to be a useful characterisation technique when evaluating the antibacterial activity of AMPs, but the experimental setup needs to be reworked in order to see an effect of the photothermal therapy.

This project has revealed important considerations to be taken into account when moving forward with research regarding AuNRs in combination with AMPs. Such a consideration would be the effect the structure of an AMP has on its antibacterial activity. It has also been shown that surfaces functionalised with photothermal AuNRs in combination with AMPs show significant antibacterial activity. A step has been made towards applying a novel method to efficiently combat BAIs without contributing to the problem of AMR.

Bibliography

[1] Marin E, Boschetto F, Pezzotti G. Biomaterials and biocompatibility: An historical overview. J Biomed Mater Res Part A. 2020;108(8):1617-33.

[2] Moriarty TF, Zaat SAJ, Busscher HJ. Biomaterials Associated Infection: Immunological Aspects and Antimicrobial Strategies. New York City, New York: Springer; 2012.

[3] Spector M. Biomedical materials to meet the challenges of the aging epidemic. Biomed Mater. 2018 Mar;13(3):030201.

[4] Pabinger C, Lothaller H, Portner N, Geissler A. Projections of hip arthroplasty in OECD countries up to 2050. HIP Int. 2018;28(5):498-506.

[5] Riool M, Zaat SAJ. In: Soria F, Rako D, de Graaf P, editors. Biomaterial-Associated Infection: Pathogenesis and Prevention. Cham: Springer International Publishing; 2022. p. 245-57.

[6] Murray CJL, Ikuta KS, Sharara F, Swetschinski L, Robles Aguilar G, Gray A, et al. Global burden of bacterial antimicrobial resistance in 2019: a systematic analysis. Lancet. 2022;399(10325):629-55.

[7] Sheridan M, Winters C, Zamboni F, Collins MN. Biomaterials: Antimicrobial surfaces in biomedical engineering and healthcare. Curr Opin Biomed Eng. 2022;22:100373.

[8] Huang X, Jain PK, El-Sayed IH, El-Sayed MA. Plasmonic photothermal therapy (PPTT) using gold nanoparticles. Lasers Med Sci. 2008;23(3):217-28.

[9] Xuan J, Feng W, Wang J, Wang R, Zhang B, Bo L, et al. Antimicrobial peptides for combating drug-resistant bacterial infections. Drug Resist Updates. 2023;68:100954.

[10] Zasloff M. Antimicrobial peptides of multicellular organisms. Nat. 2002;415(6870):389-95.

[11] Williams DF. On the nature of biomaterials. Biomaterials. 2009;30(30):5897-909.

[12] Zhang X, Williams D. Definitions of Biomaterials for the Twenty-First Century. Materials Today. Amsterdam, Netherlands: Elsevier; 2019.

[13] Pietrocola G, Campoccia D, Motta C, Montanaro L, Arciola C, Speziale P. Colonization and Infection of Indwelling Medical Devices by Staphylococcus aureus with an Emphasis on Orthopedic Implants. Int J Mol Sci. 2022;23(11):5958.

[14] Lowy FD. *Staphylococcus aureus* Infections. N Engl J Med. 1998;339(8):520-32.

[15] Abushaheen MA, Muzaheed, Fatani AJ, Alosaimi M, Mansy W, George M, et al. Antimicrobial resistance, mechanisms and its clinical significance. Dis Mon. 2020;66(6):100971.

[16] Petryayeva E, Krull UJ. Localized surface plasmon resonance: Nanostructures, bioassays and biosensing—A review. Anal Chim Acta. 2011;706(1):8-24.

[17] Huang X, Neretina S, El-Sayed MA. Gold Nanorods: From Synthesis and Properties to Biological and Biomedical Applications. Adv Mater. 2009;21(48):4880-910.

[18] Uusitalo M, Eriksson G, Hulander M, Andersson M. Gold Nanorods as Photothermal Antibacterial Materials. ACS Appl Nano Mater. 2025;8(7):3661-70.

[19] Kazemzadeh-Narbat M, Cheng H, Chabok R, Alvarez MM, de la Fuente-Nunez C, Phillips KS, et al. Strategies for antimicrobial peptide coatings on medical devices: a review and regulatory science perspective. Crit Rev Biotechnol. 2021;41(1):94-120.

[20] Yeung ATY, Gellatly SL, Hancock REW. Multifunctional cationic host defence peptides and their clinical applications. Cell Mol Life Sci. 2011;68(13):2161-76.

[21] Stepulane A, Rajasekharan AK, Andersson M. Antibacterial efficacy of antimicrobial peptide-functionalized hydrogel particles combined with vancomycin and oxacillin antibiotics. Int J Pharm. 2024;664:124630.

[22] Jazayeri MH, Amani H, Pourfatollah AA, Pazoki-Toroudi H, Sedighimoghaddam B. Various methods of gold nanoparticles (GNPs) conjugation to antibodies. Sens Bio-Sens Res. 2016;9:17-22.

[23] Kadeřábková N, Mahmood AJS, Mavridou DAI. Antibiotic susceptibility testing using minimum inhibitory concentration (MIC) assays. npj Antimicrob Resist. 2024;2(1).

[24] Wiegand I, Hilpert K, Hancock REW. Agar and broth dilution methods to determine the minimal inhibitory concentration (MIC) of antimicrobial substances. Nat Protoc. 2008;3(2):163-75.

[25] Muralimohan A, Eun YJ, Bhattacharyya B, Weibel DB. Dissecting microbiological systems using materials science. Trends Microbiol. 2009;17(3):100-8.

[26] Uusitalo M, Eriksson G, Hulander M, Andersson M. Gold Nanorods as Photothermal Antibacterial Materials. ACS Appl Nano Mater. 2025;8(7):3661-70.

[27] Zhao W, Sachsenmeier K, Zhang L, Sult E, Hollingsworth RE, Yang H. A New Bliss Independence Model to Analyze Drug Combination Data. J Biomol Screen. 2014;19(5):817-21.

[28] Berenbaum MC. Synergy, additivism and antagonism in immunosuppression. A critical review. Clin Exp Immunol. 1977;28(1):1-18.

[29] Zhang Q, Li RX, Chen X, He XX, Han AL, Fang GZ, et al. Study of Efficiency of Coupling Peptides with Gold Nanoparticles. Chin J Anal Chem. 2017;45(5):662-7.

[30] Thermofischer Scientific Inc. Carbodiimide Crosslinker Chemistry [Internet]. Waltham, Massachusetts: Thermofischer Scientific Inc; 2025 [cited 2025 June 6]. Available from: `https://www.thermofisher.com/se/en/home/life-science/protein-biology/protein-biology-learning-center/protein-biology-resource-library/pierce-protein-methods/carbodiimide-crosslinker-chemistry.html`.

[31] Lichtman JW, Conchello JA. Fluorescence microscopy. Nat Methods. 2005;2(12):910-9.

[32] Stiefel P, Schmidt-Emrich S, Maniura-Weber K, Ren Q. Critical aspects of using bacterial cell viability assays with the fluorophores SYTO9 and propidium iodide. BMC Microbiol. 2015;15(1):36.

[33] Schindelin J, Arganda-Carreras I, Frise E, Kaynig V, Longair M, Pietzsch T, et al. Fiji: an open-source platform for biological-image analysis. Nat Methods. 2012;9(7):676-82.

[34] OriginLab Corporation. Origin and OriginPro [Internet]. Northampton, Massachusetts: OriginLab Corporation; 2025 [cited 2025 May 31]. Available from: `https://www.originlab.com/index.aspx?go=PRODUCTS/Origin`.

[35] Xu M, Fralick D, Zheng JZ, Wang B, Tu XM, Feng C. The Differences and Similarities Between Two-Sample T-Test and Paired T-Test. Shanghai Arch Psychiatry. 2017;29(3):184-8.

A

Appendix 1

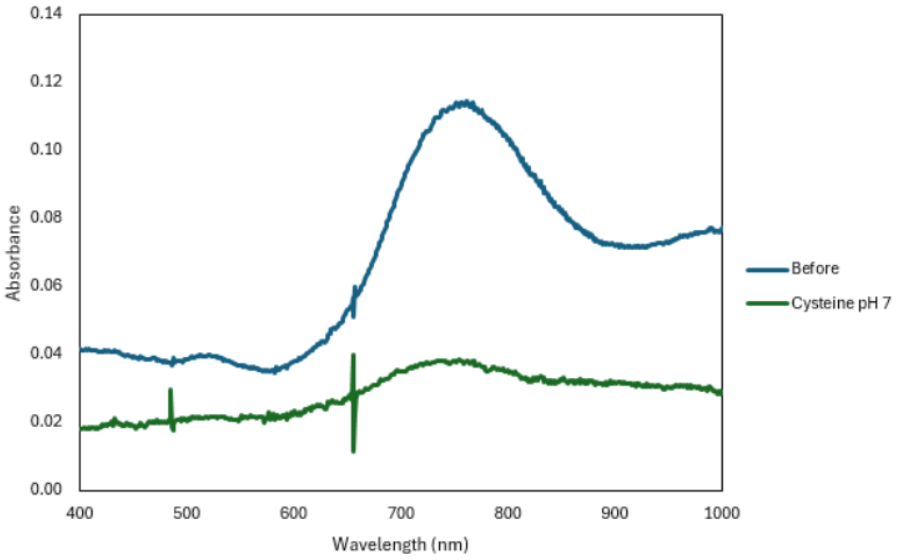

Figure 13: Absorbance spectrum of a sample of AuNR functionalised glass, showcasing absorbance before and after the surface was immersed in 1 mM of cysteine.

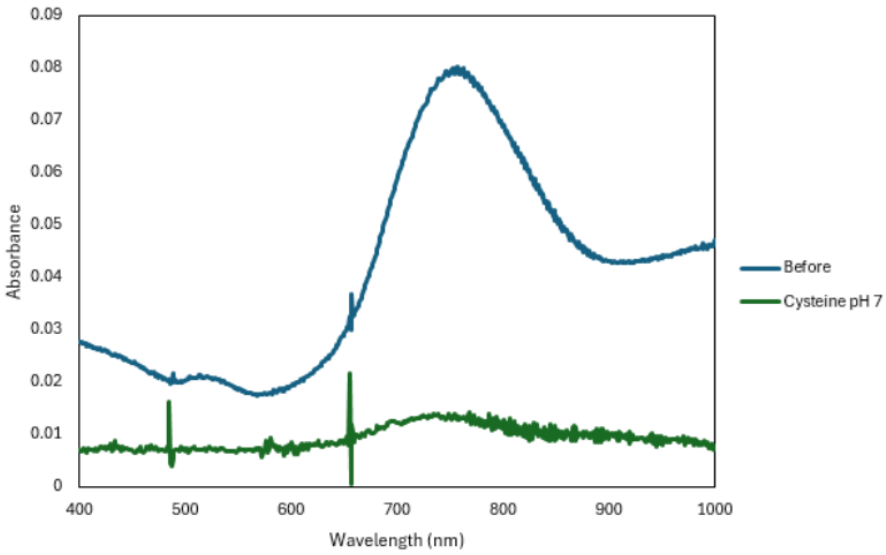

Figure 14: Absorbance spectrum of a sample of AuNR functionalised glass, showcasing absorbance before and after the surface was immersed in 1 mM of cysteine.

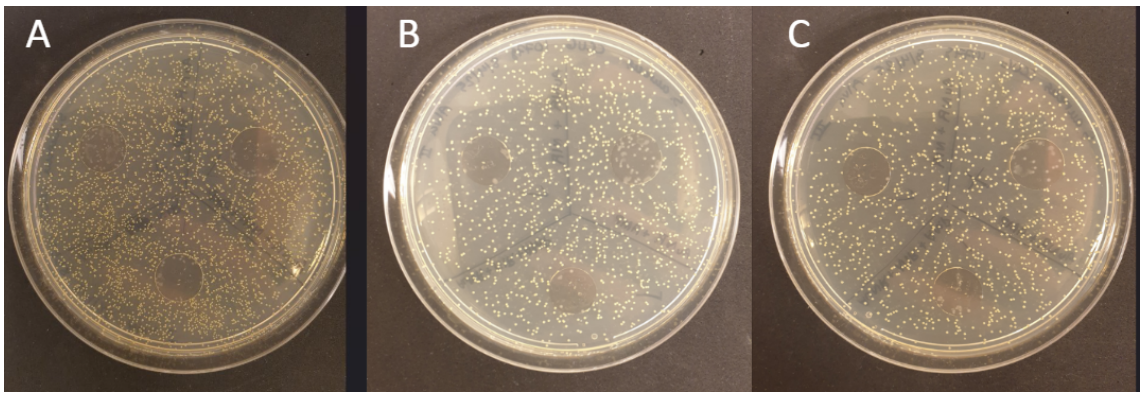

Figure 15: Three MH-agar plates streaked with the same suspension of *S. aureus* showcasing differing cell density depending on which order they were streaked in. (A) the first plate streaked, (B) the second plate streaked and (C) the third plate streaked.

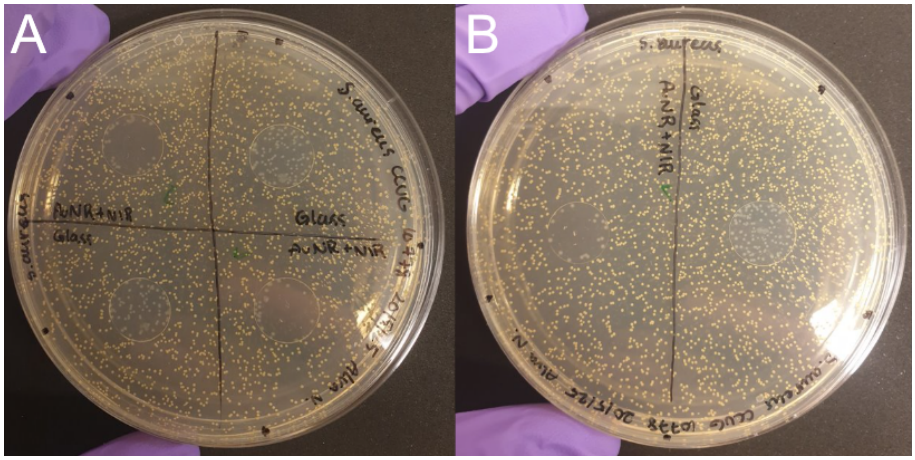

Figure 16: Two MH-agar plates streaked with the same suspension of *S. aureus* showcasing similar cell density independent of which order they were streaked in. (A) the first plate streaked and (B) the second plate streaked.

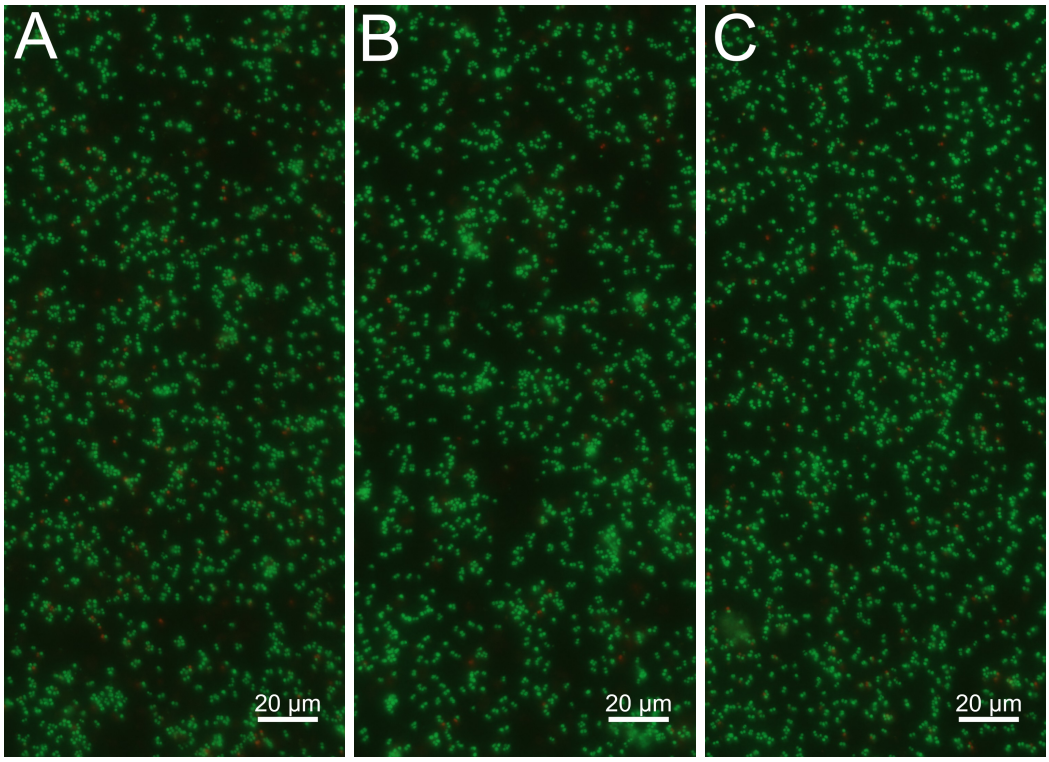

Figure 17: Fluorescence microscopy micrographs of LIVE/DEAD® BacLight™ stained *S. aureus* grown on (A) a glass surface immersed in 3.125 µM RRP9W4N AMP for one hour, (B) a AuNR functionalised glass surface irradiated with 14 W/cm^2 NIR light for 30 seconds and (C) a AuNR functionalised glass surface irradiated with 14 W/cm^2 NIR light for 30 seconds and immersed in 3.125 µM RRP9W4N AMP for one hour.

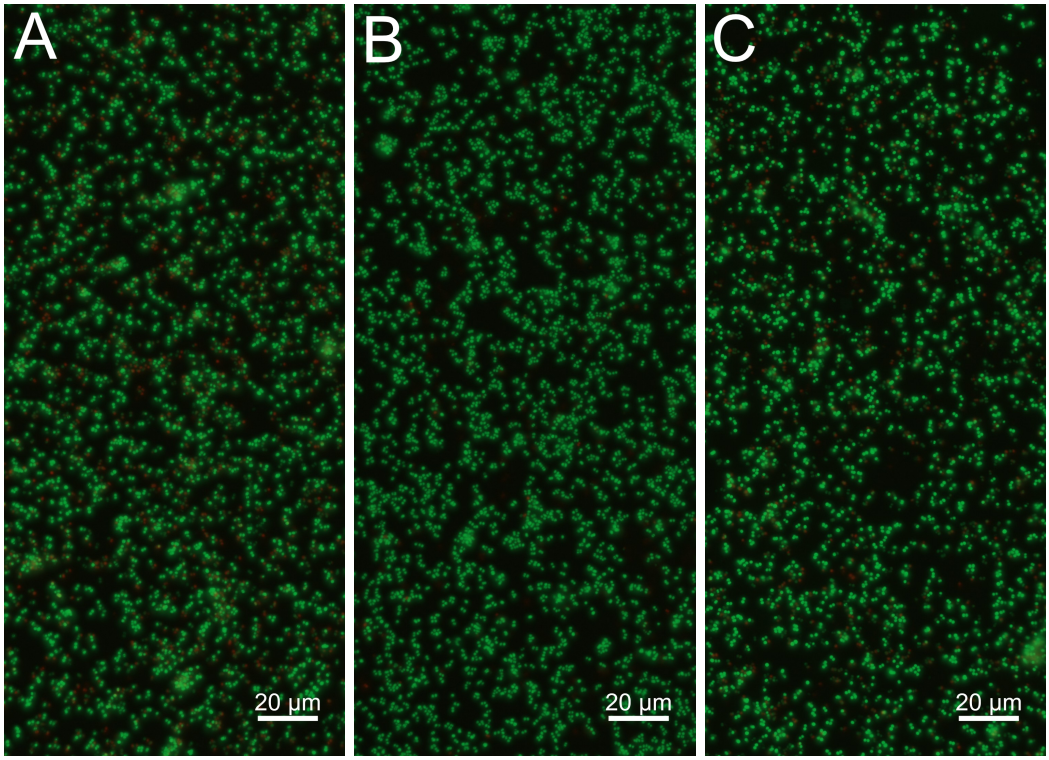

Figure 18: Fluorescence microscopy micrographs of LIVE/DEAD® BacLight™ stained *S. aureus* grown on (A) a glass surface immersed in 6.25 µM RRP9W4N AMP for one hour, (B) a AuNR functionalised glass surface irradiated with 16 W/cm^2 NIR light for 30 seconds and (C) a AuNR functionalised glass surface irradiated with 16 W/cm^2 NIR light for 30 seconds and immersed in 6.25 µM RRP9W4N AMP for one hour.

DEPARTMENT OF CHEMISTRY AND CHEMICAL ENGINEERING
CHALMERS UNIVERSITY OF TECHNOLOGY
Gothenburg, Sweden
www.chalmers.se

CHALMERS
UNIVERSITY OF TECHNOLOGY